Int. J. Electrochem. Sci., 7 **(2012)** 9478 - 9487

International Journal of
ELECTROCHEMICAL
SCIENCE
www.electrochemsci.org

Collection Efficiency Enhancement of Injected Electrons in Dye-sensitized Solar Cells with a Ti Interfacial Layer and $TiCl_4$ Treatment

Yu-Hsien Lin[1,*] , *Yung-Chun Wu*[2], *Bo-Yu Lai*[2]

[1] Department of Electronic Engineering, National United University, Miaoli, Taiwan
[2] Department of Engineering and System Science, National Tsing Hua University, Hsinchu, Taiwan
[*]E-mail: yhlin@nuu.edu.tw

Received: 9 August 2012 / *Accepted:* 4 September 2012 / *Published:* 1 October 2012

This study attempts to enhance the performance of dye-sensitized solar cells (DSSCs) by integrating $TiCl_4$ treatment on porous TiO_2 and the Ti-deposited thin film metal on FTO. The electron conductance of the interface between the FTO glass and the electron transport on the porous TiO_2 film can be improved by sputtering the Ti interfacial layer. The modified DSSCs achieve significantly better short-circuit photocurrent density (J_{sc}), approximately 42% greater than that of the standard cell. This ultimately produces a 6.13% energy conversion efficiency (η), which is approximately 33% higher than that of a standard cell. The incident monochromatic photon-to-current conversion efficiency (IPCE) spectra of the modified DSSCs show a higher value than that of a standard cell, especially in the higher wavelength range.

Keywords: Dye-sensitized solar cell, $TiCl_4$ treatment, counter electrode, collection efficiency, excited electron

1. INTRODUCTION

Dye-sensitized solar cells (DSSCs) [1] are promising alternatives to silicon-based solar cells [2] because of their environmental friendliness, low manufacturing costs, and flexibility. Researchers have recently devoted considerable efforts to increasing the light harvesting efficiency (LHE) of photoelectrodes to achieve high photovoltaic performance.

Increasing the absorption path length of photons by light scattering is a conventional means of improving LHE [3-13]. Adding large particles as scattering layers improves absorption [8]. Light scattering can be enhanced by multilayer cells, which consist of TiO_2 particles of various sizes [10]. Previous research has also discussed mixing TiO_2 particles with TiO_2-Rutile and ZrO_2 as scattering

layers [12].

Another way to improve LHE is to improve the collection efficiency of the injected electrons using FTO. The electrical conductance and the surface connection of the porous TiO_2 photoelectrode [14,15] is likely the key subject. A well-known method is to use a thin TiO_2 film or metal thin film as the blocking layer to improve the interfacial conductance between the FTO glass and the porous TiO_2 film, preventing the back reaction of electrons with tri-iodide ions in the electrolyte and oxidized dye [16]. Sputtering titanium (Ti) thin film on the FTO glass to form a blocking layer can prevent the reverse reaction [17]. Non-noble metal grids of Ni, Cu, and Al can also be used to enhance the interfacial conductance [18]. Other researchers have reported depositing fine TiO_2 membranes by spray pyrolysis [19], and dense TiO_2 thin-film formed by chemical vapor deposition [20].

This study proposes the integration of a sputtered Ti interfacial layer method and $TiCl_4$ treatment on DSSCs. According to previous studies, $TiCl_4$ treatment enhances the connection between TiO_2 particles [21], increases the diameter of TiO_2 particles [22,23], and even improves the dye loading [22]. The interfacial layer should also consider the contact resistance, the work function match, and the transmittance. This study uses a 10 nm titanium metal film deposited on FTO, which has a work function of 4.33 eV titanium, to improve the electron conductance of the interface between the FTO glass and the porous TiO_2, and increase the electron transport on the porous TiO_2 film.

2. EXPERIMENTAL DETAILS

Figure 1 shows a schematic diagram of the modified DSSCs with a Ti interfacial layer over FTO and the $TiCl_4$ treatment on the photoelectrode. The Ti thin film was deposited by DC sputtering using Ti targets on FTO glass. The Ar flow and power were kept constant at 24 sccm and 150 W, respectively. The deposition thickness was 10 nm.

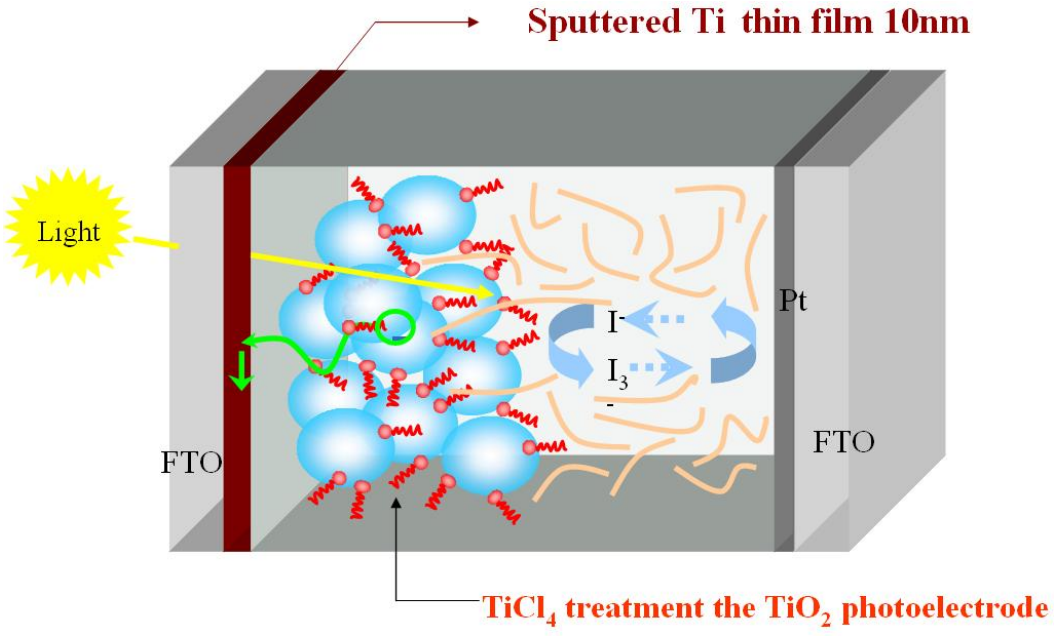

Figure 1. Schematic of modified DSSCs with sputtered Ti thin film over FTO and $TiCl_4$ treatment on the photoelectrode.

Colloidal TiO_2 paste was prepared using Degussa P25 powder mixed Triton X-I00, acetylacetone, polyethylene glycol, and DI-water. The paste was spread on the FTO glass. After drying in an oven at 120 °C, the electrode was sintered for 30 min at 450 °C in air. The resulting film thickness was 12 μm, and the effective area was 0.25 cm^2. $TiCl_4$ treatment was then applied to the prepared TiO_2 films. The sintered TiO_2 films were dipped in an aqueous solution of 50 mM $TiCl_4$ at 70 °C for 30 min, and sintered again for 30 min at 450 °C. The sintered TiO_2 electrode was then immersed for 24 h in a 3×10^{-4} M ethanol solution of the dye, N719.

The counter electrode was prepared on a bare FTO substrate. The Pt precursor was prepared by H_2PtCl_6, and spread on the front side of the FTO glass. The electrolyte consisted of 0.1 M LiI, 0.03 M I_2, and 0.5M 4-tert-buytylpyridine in 3-methoxypropionitrile.

3. RESULTS AND DISCUSSION

Figure 2 shows the current density-voltage (J-V) characteristics of the DSSCs of the FTO and FTO/Ti substrate, and with $TiCl_4$ treatment on the photoelectrode. These results were measured under 100 mW/cm^2 irradiation by a solar simulator. Table 1 presents a summary of the important photovoltaic characteristics and parameters. The average characteristic values, including the short-circuit photocurrent density (J_{sc}), open-circuit voltage (V_{oc}), and fill factor (FF) of the FTO standard cell are 9.37 mA/cm^2, 0.73 V, and 0.66, corresponding to a conversion efficiency of 4.61%. After the Ti thin film was deposited on the FTO substrate, the device exhibited a great improvement conversion efficiency of 5.31%, which is approximately 15% higher than a standard cell. The average photovoltaic characteristic of J_{sc}, V_{oc}, and FF for the $TiCl_4$-treated DSSCs are 11.54 mA/cm^2, 0.73 V, and 0.63, respectively. The $TiCl_4$ treatment was also applied to a DSSC based on FTO/Ti substrate, achieving a higher short-circuit photocurrent density of 13.28%. Finally, the DSSC with $TiCl_4$ treatment and the Ti interfacial layer shows a 6.13% has higher energy conversion efficiency.

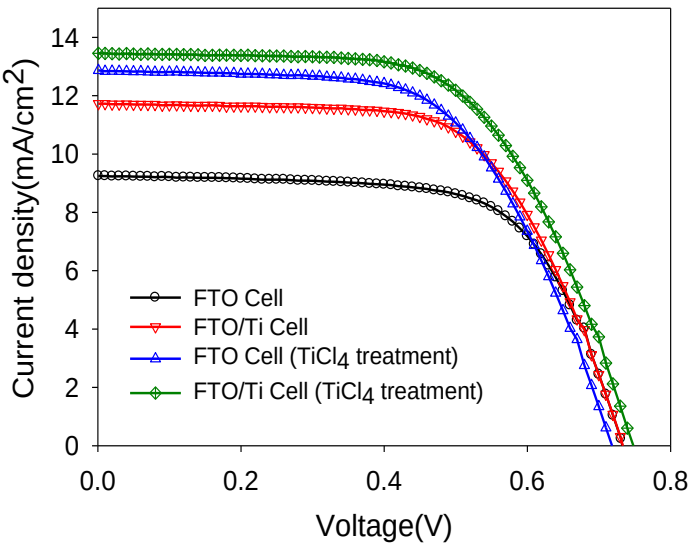

Figure 2. Photocurrent-voltage (J-V) characteristics of the DSSCs of FTO and FTO/Ti substrate, and with $TiCl_4$ treatment on the photoelectrode.

Table I Photovoltaic parameters of the DSSCs of FTO and FTO/Ti substrate, and with $TiCl_4$ treatment on the photoelectrode.

	η(%)	FF	J_{sc}(mA/cm2)	Voc(V)
FTO STD Cell	4.61(±0.10)	0.66	9.37(±0.11)	0.73
FTO/Ti Cell	5.31(±0.08)	0.63	11.54(±0.13)	0.73
FTO Cell ($TiCl_4$)	5.59(±0.15)	0.60	13.02(±0.46)	0.72
FTO/Ti Cell ($TiCl_4$)	6.13(±0.02)	0.61	13.28(±0.15)	0.75

Figure 3 shows the scanning electron microscope (SEM) surface morphologies of porous TiO_2 films with and without $TiCl_4$ treatment. Figure 3(a) shows that the untreated TiO_2 has particle diameters of approximately 25 nm. After $TiCl_4$ treatment, the TiO_2 particles increased in diameter (Fig. 3(b)). For the enlarged area of the surface morphology of the treated porous TiO_2, the maximum diameter was approximately 250 nm. Moreover, the formation of large particles ensured greater light harvesting in the photoelectrode because of light scattering.

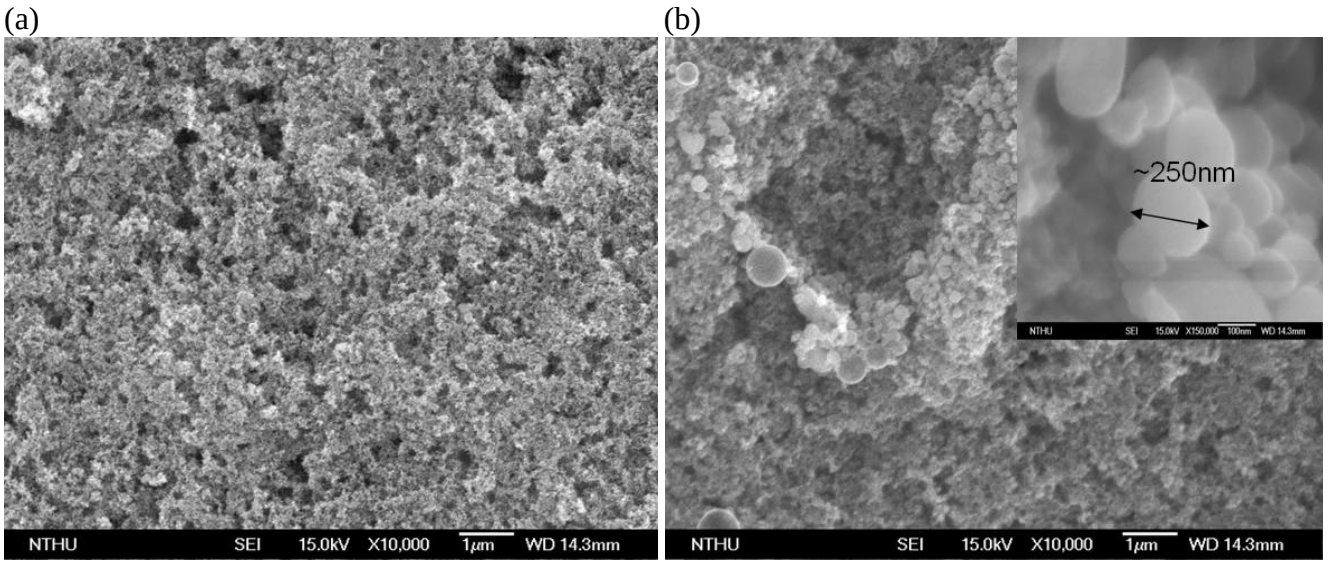

Figure 3. SEM photographs of (a) standard porous TiO_2 films, (b) with $TiCl_4$ treatment.

Figure 4 presents the XPS analysis of the FTO/Ti substrate after it was sintered for 30 min at 450 °C in air. Figure 4(a) shows the curve-fitted XPS spectra of the Ti 2p regions: only the Ti^{4+} (464.7 and 459.0 eV) signal is observable. Figure 4(b) shows the O 1s feature, which consists of two peaks. The strongest peak appears at 530.3 eV, and corresponds to the oxygen in O^{2-}. The second peak appears at 532 eV, and corresponds to the oxygen in OH^- groups. Curve fitting shows that the O^{2-} account for the majority of the O species. Figures 4(a) and 4(b) demonstrate the presence of Ti^{4+} and O^{2-}, and confirm that the sintered FTO/Ti forms TiO_2 on the FTO substrate.

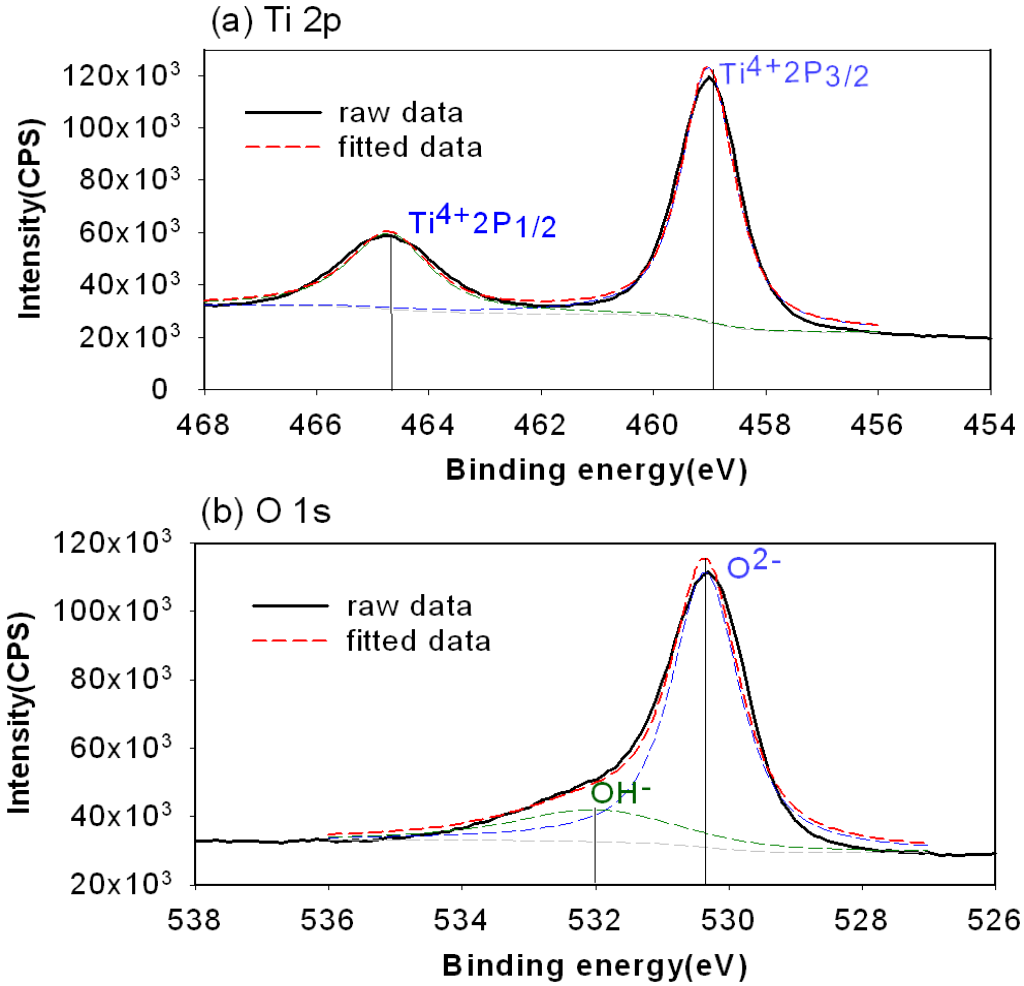

Figure 4. XPS spectra and curve fits of (a) Ti 2p and (b) O 1s of Ti on FTO/Ti after sintering.

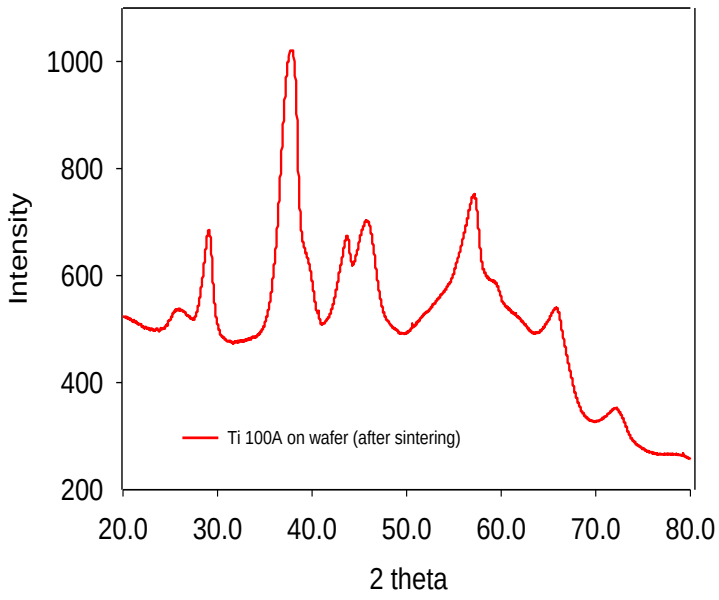

Figure 5. XRD patterns of Si wafer/Ti substrate before and after sintering at 450 °C

Figure 5 shows the XRD analysis of the Ti-sputtered wafer after it was sintered for 30 min at 450 °C in air. Because it is difficult to detect a new phase on the FTO substrate with XRD technology, the XRD analysis was measured on the Ti-sputtered wafer. The results show two peaks, the signal 26.01 eV and the signal 38.00 eV, which are in the range of the TiO_2 rutile form and the TiO_2 anatase form. This means that after 450 °C sintering, the Ti thin film was transformed into semiconductor oxide (TiO_2) with a form between that of the rutile and anatase forms. It would be a dense TiO_2 film to compare with the porous TiO_2 film, and it is suitable as a blocking layer to help electrons transport smoothly.

Figure 6 shows the energy-band diagrams of a structure with an FTO electrode, a dense TiO_2 layer, and a porous TiO_2 electrode structure (FTO/BL-TiO_2/TiO_2). The work function (ϕ) of FTO is 4.4 eV [24]. The electron affinity (χ) and work function of the porous anatase n-type semiconductor TiO_2 are 4.1 eV and 4.2 eV, respectively [25,26]. The dense TiO_2 layer is between the anatase and the rutile form, and the electron affinity of the dense TiO_2 layer is a little higher than the anatase structure porous TiO_2 of 4.1 eV, but lower than the rutile form TiO_2. Thus, this dense TiO_2 layer forms a proper conduction band offset. These results show that the excited electrons can transport from the porous TiO_2 to the FTO substrate smoothly because of the work function match of the dense TiO_2 layer. This work likes an electron blocking layer (BL), and can also prevent the electrons from reacting with the electrolyte and excited dye. Therefore, Ti-deposited DSSC has a higher J_{sc} and efficiency than the standard cell.

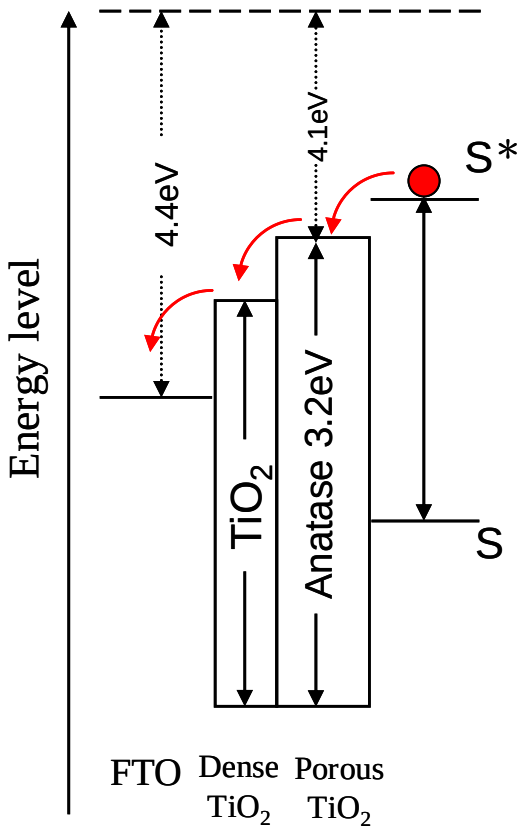

Figure 6. Energy-band diagrams of FTO/Dense-TiO_2/TiO_2/Dye.

Figure 7 shows the impedance spectra of DSSCs with and without $TiCl_4$ treatment in the complex plane. Z_1 and Z_2 are the impedances related to charge-transfer processes at the surface of the CE and at the TiO_2/dye/electrolyte interface, respectively. The resistances of each impedance (Z_1 and Z_2) for the standard DSSC are 11.7 and 28.7 Ωcm^2, and the resistances related to each impedance (Z_1 and Z_2) of the $TiCl_4$-treated DSSC are 11.6 and 27.7 Ωcm^2, respectively. After $TiCl_4$ treatment, the impedance in the second semi-circle (Z_2) decreases apparently. The $TiCl_4$ treatment can enhance the connection of TiO_2 particles, enhancing the charge transportation through the TiO_2 electrode.

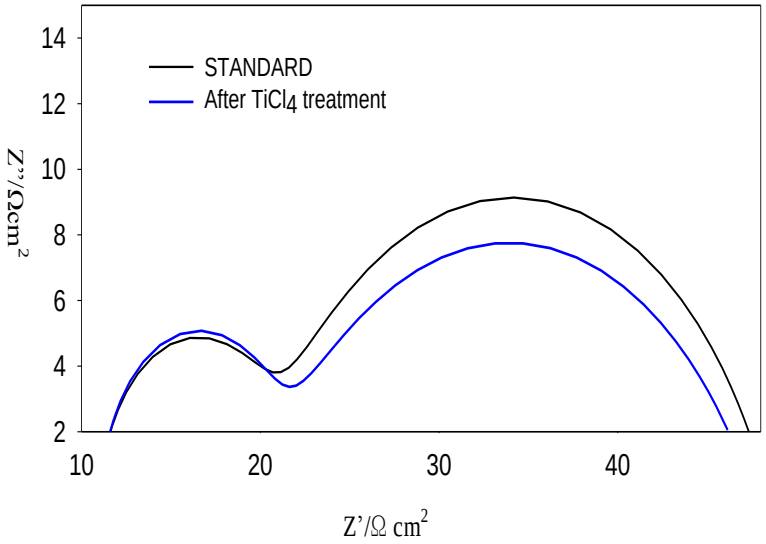

Figure 7. Electrochemical impedance spectra of DSSC with and without $TiCl_4$ treatment under illumination.

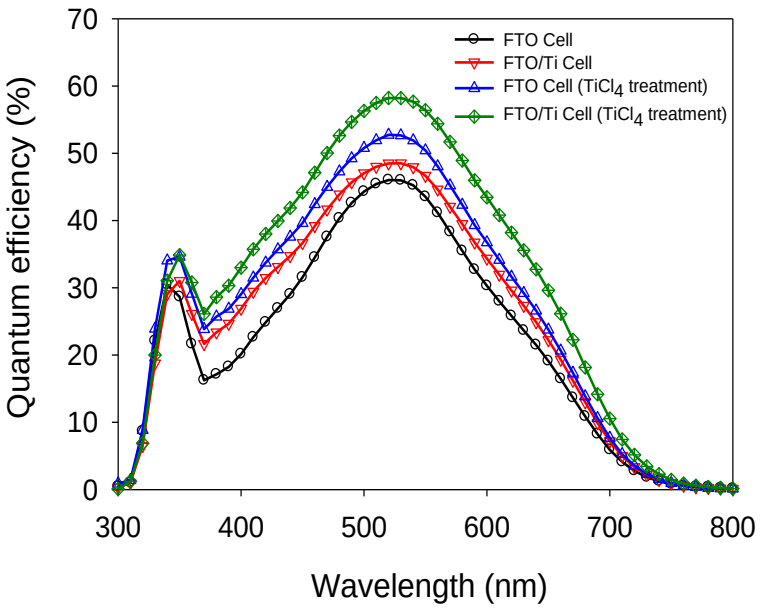

Figure 8. IPCE spectra for the DSSCs of FTO and FTO/Ti substrate, and with $TiCl_4$ treatment on the photoelectrode.

Figure 8 shows the IPCE spectra for the DSSCs of FTO and FTO/Ti substrates and with $TiCl_4$ treatment on the photoelectrode. After the Ti interfacial layer was deposited on the FTO substrate, the cells raise the IPCE compared to the IPCE of FTO-based cells in the whole wavelength. Similarly, the $TiCl_4$-treated cells also raise the IPCE curve compared to the IPCE of untreated cells. Because the Ti interfacial layer and the $TiCl_4$ treatment technologies were both integrated using in the DSSC, the IPCE curve presents the highest value in the whole wavelength.

Generally, J_{sc} can be expressed using the following equation [10];

$$J_{sc} = \int q \cdot F(\lambda) \cdot [1-r(\lambda)] . IPCE(\lambda) d\lambda \qquad (1)$$

where q denotes the electron charge, F(λ) denotes the incident photon flux density at wavelength λ, and $r(\lambda)$ denotes the loss of the incident light by the light absorption and reflection of the FTO glass. Three other factors also influence IPCE(λ), and their correlation is given by the following equation [27];

$$IPCE(\lambda) = LHE(\lambda) \cdot \varphi_{inj} \cdot \eta_{coll} \qquad (2)$$

where LHE(λ) denotes the light harvesting efficiency of the dye absorbed, φ_{inj} denotes the injection efficiency of the electron from the excited dye into the TiO_2, and η_{coll} denotes the collection efficiency of the injected electrons by the FTO. This study adopts φ_{inj} with an identical value because of the identical dye (N719) used. The $TiCl_4$-treated cells enhanced the dye loading of the TiO_2 film and light scattering, explaining the increase of the LHE(λ) of the $TiCl_4$-treated cells.

Conversely, η_{coll} can be estimated using the transport (k_t) rate and the recombination (k_r) rate as $\eta_{coll} \sim k_t/(k_t + k_r)$ [28]. Because the $TiCl_4$-treated cells improve the connection between TiO_2 particles, the treated cells enhance the transport rate and decrease the recombination rate of excited electrons [16]. Therefore, the overall IPCE after $TiCl_4$ treatment is higher than that of the untreated cell. The Ti thin film can supply the dense TiO_2 film with an interfacial layer, and may reconstruct the interface between the FTO substrate and the porous TiO_2 film. The Ti thin film can also be used as a blocking layer to improve electron conduction and suppress interfacial electron recombination. Therefore, the term η_{coll} in the IPCE equation increases with the enhancement of the rate for transport (k_t) and decreases with the recombination (k_r) rate.

Thus, applying $TiCl_4$ treatment to porous TiO_2 and applying the Ti-deposited thin film metal on FTO can achieve a higher LHE(λ), φ_{inj}, and η_{coll} value, which in turn improves the IPCE and J_{sc} values.

4. CONCLUSIONS

In summary, this study reports the successful application of $TiCl_4$ treatment to porous TiO_2 and the Ti-deposited thin film metal on FTO to improve the performance of DSSCs. After sintering, Ti oxidizes to form TiO_2 and serves as a blocking layer to prevent back reaction. This also increases the electron conduction and suppresses the interfacial electrons recombination because of conduction band

matching. $TiCl_4$ treatment enhances the transport of excited electrons on the porous TiO_2. These processes are simple and cost-effective, and can be integrated in current DSSCs with glass or flexible substrates.

ACKNOWLEDGMENTS
This study was sponsored by the National Science Council, Taiwan, under Contract No. 101-2221-E-239-026-. The National Nano Device Laboratories (NDL) is also greatly appreciated for its technical support.

References

1. B.O'Regan and M. Gratzel, *Nature*, 353 (1991) 737.
2. H. Tsubomura, M. Matsumura, Y. Nomura, and T. Amamiya, *Nature*, 261 (1976) 402.
3. Nada F. Atta, Hatem M.A. Amin, Mohamed W. Khalil, and Ahmed Galal, *Int. J. Electrochem. Sci*., 6 (2011) 3316.
4. Tsung-Hsuan Tsai, Shr-Chiang Chiou, Shen-Ming Chen, and Kuo-Chiang Lin, *Int. J. Electrochem. Sci.*, 6 (2011) 3938.
5. Zhen Wei, Yu Yao, Tao Huang, and Aishui Yu, *Int. J. Electrochem. Sci*., 6 (2011) 1871.
6. Jo-Lin Lan, Chi-Chao Wan, Tzu-Chien Wei, Wen-Chi Hsu, Chao Peng, Ya-Huei Chang, and Chih-Ming Chen, *Int. J. Electrochem. Sci*., 6 (2011) 1230.
7. M. H. Lai, M. W. Lee, Gou-Jen Wang and M. F. Tai, *Int. J. Electrochem. Sci*., 6 (2011) 2122.
8. J. Ferber and J. Luther, *Sol. Energy Mater. Sol. Cells*, 54 (1998), 265.
9. A. Usami, *Sol. Energy Mater. Sol. Cells*, 64 (2000) 73.
10. Z.-S. Wang, H. Kawauchi, T. Kashima, and H. Arakawa, *Coord. Chern. Rev*., 248 (2004) 1381.
11. J.-K. Lee, B.-H. Jeong, S.-1. Jang, Y.-G. Kim, Y.-W. Jang, S.-B. Lee, and M.-R. Kim, *J. Ind. Eng. Chern.* 15 (2009) 724.
12. S. Hore, C. Vetter, R. Kern, H. Smit, and A. Hinsch, *Sol. Energy Mater. Sol. Cells*, 90 (2006) 1176.
13. Z. Tian, H. Tian, X. Wang, S. Yuan, J. Zhang, X. Zhang, T. Yu, and Z. Zou, *Appl. Phys. Let*t., 94 (2009) 031905.
14. Cao F, Oskam G, Meyer G, Searson P, *J. Phys. Chem*. B 100 (1996) 17021.
15. Solbrand A et al., *J. Phys. Chem*. B 101 (1997) 2514.
16. Petra J. Cameron and Laurence M. Peter, *J. Phys. Chem*. B 107 (2003) 14394.
17. Jiangbin Xia, Naruhiko Masaki, Kejian Jiang, and Shozo Yanagida, *J. Phys. Chem*. B 110 (2006) 25222.
18. S. H. Seo, H. J. Kim, B. K. Koo, D. Y. Lee, *J. Electrochem. Soc*. 156 (2009) 128.
19. J. Krüger, R. Plass, L. Cevey, M. Piccirelli, M. Grätzel, *Appl. Phys. Lett*. 79 (2001), 2085.
20. H. Yamashita, Y. Ichihashi, M. Harada, G. Stewart, M.A. Fox, M. Anpo, *J. Catal*. 158 (1996) 97.
21. 21 M.-Y. Song, D.-K. Kim, S.-M. Jo, and D.-Y. Kim, *Synth. Met*., 155 (2005) 635.
22. P. M. Sommeling, B. C. O'Regan, R. R. Haswell, H. J. P. Smit, N. J. Bakker, J. J. T. Smits, J. M. Kroon, and J. A. M. van Roosmalen, *J. Phys. Chern*. B, 110 (2006) 19191.
23. N. Fuke, R. Katoh, A. Islam, M. Kasuya, A. Furube, A. Fukui,Y. Chiba, R. Komiya, R. Yamanaka, L. Han, and H. Harimac, *Energy Environ. Sci*., 2 (2009) 1205.
24. A. Andersson, N. Johansson, P. BrGms, N. Yu, D. Lupo, and W. R. Salaneck, *Adv. Mater*. 10 (1998) 859..
25. Amy L. Linsebigler, Guangquan Lu, John T. Yates, *Chem. Rev*. 95 (1995) 735.
26. Grätzel, M. *Nature* 414 (2001) 338.
27. M.K. Nazeeruddin, P. Pechy, T. Renouard, S.M. Zakeeruddin, R Humphry-Baker, P. Comte, P. Liska, L. Cevey, E. Costa, V. Shklover, L. Spiccia, G.B. Deacon, C.A. Bignozzi, and M. Gratzel, *J.*

Am. Chern. Soc., 123 (2001) 1613.
28. K.Hara, H. Sugihhara,Y. Tachibana, A. Islam, M. Yanagida, K. Sayama, and H. Arakawa, *Langmuir*, 17 (2001) 5992.